THE JOURNAL OF PHYSICAL CHEMISTRY A

Article

pubs.acs.org/JPCA

A Multireference Configuration Interaction Study of the Photodynamics of Nitroethylene

Itamar Borges, Jr.,*[,†] Adélia J. A. Aquino,[‡,§] and Hans Lischka*[,‡,∥]

[†]Departamento de Química, Instituto Militar de Engenharia Praça General Tibúrcio, 80, 22290-270 Rio de Janeiro, Brazil

[‡]Department of Chemistry and Biochemistry, Texas Tech University, Lubbock, Texas 79409, United States

[§]Institute of Soil Research, University of Natural Resources and Life Sciences Vienna, Peter-Jordan-Straße 82, A-1190 Vienna, Austria

[∥]Institute for Theoretical Chemistry, University of Vienna, Währingerstrasse 17, A-1090 Wien, Austria

Supporting Information

ABSTRACT: Extended multireference configuration interaction with singles and doubles (MR-CISD) calculations of nitroethylene ($H_2C{=}CHNO_2$) were carried out to investigate the photodynamical deactivation paths to the ground state. The ground (S_0) and the first five valence excited electronic states (S_1–S_5) were investigated. In the first step, vertical excitations and potential energy curves for CH_2 and NO_2 torsions and CH_2 out-of-plane bending starting from the ground state geometry were computed. Afterward, five conical intersections, one between each pair of adjacent states, were located. The vertical calculations mostly confirm the previous assignment of experimental spectrum and theoretical results using lower-level calculations. The conical intersections have as main features the torsion of the CH_2 moiety, different distortions of the NO_2 group and CC, CN, and NO bond stretchings. In these conical intersections, the NO_2 group plays an important role, also seen in excited state investigations of other nitro molecules. Based on the conical intersections found, a photochemical nonradiative deactivation process after a π–π^* excitation to the bright S_5 state is proposed. In particular, the possibility of NO_2 release in the ground state, an important property in nitro explosives, was found to be possible.

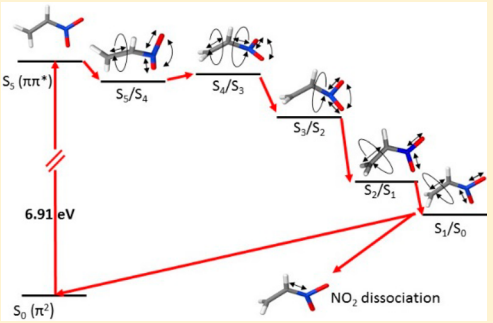

1. INTRODUCTION

The explosophore NO_2 group is an essential component in many propellants and explosives of practical relevance.[1] These nitro compounds are usually thermally unstable, composed of easily broken N–N, O–C and C–N covalent bonds, have significant biological activity, and may contribute to atmospheric pollution.[2] Furthermore, decomposition processes of nitro compounds are especially important because they occur at relatively low temperatures and are involved in the detonation of explosives.[3,4]

Most of the energetic molecules have diffuse electronic spectra and propensity to dissociate and rearrange.[5] In the detonation initiation of these materials, photochemical processes are very important.[6−12] In particular, as has been increasingly recognized in the field of photochemical reactions,[13,14] nonradiative decomposition processes of energetic molecules through conical intersections play an important and even dominant role.[15−17] Therefore, investigations of nonadiabatic processes occurring in energetic molecules are especially interesting.

The study of gas phase energetic molecules can unveil their properties and reactions at the molecular level, and determine decomposition features as a function of the electronic and vibrational excitations.[7] However, the experimental measurements of decomposition processes and their interpretation are very complex, a picture asking for theoretical investigations. Moreover, in spite of the importance of excited states in energetic materials research, only few studies have been carried out in this field.[6,17]

We recently investigated the electronic excitation spectra of energetic molecules containing nitro groups, namely, nitramide (H_2NNO_2),[18] *N*,*N*-dimethylnitramine, ($(CH_3)_2NNO_2$),[19] 1,1-diamino-2,2-dinitroethylene (FOX-7 or DADNE),[20] and hexahydro-1,3,5-trinitro-1,3,5-triazine (RDX).[21] These molecules are building blocks of energetic materials and bear easily broken N–NO_2 bonds. Nitroethylene ($H_2C{=}CHNO_2$) and FOX-7, in contrast with the other studied molecules, have a C–NO_2 bond instead of a N–NO_2. These C–NO_2 bonds are also relatively weak and have its NO_2 group adjacent to a C=C bond.

Nitroethylene is the simplest member of the nitro-olefin series. This molecule displays conjugation effects between the ethylenic π electrons and those on the nitro group[22] that affect the electronic spectrum. Molecules of this class are potentially synthetic reagents, powerful electron acceptors due to the

Special Issue: David R. Yarkony Festschrift

Received: July 23, 2014
Revised: August 25, 2014
Published: August 26, 2014

   dx.doi.org/10.1021/jp507396e | J. Phys. Chem. A 2014, 118, 12011−12020

presence of NO_2 groups, and can also behave as precursors to useful polymers and copolymers for explosives technologies.[3]

In spite of the variety of aforementioned interests, previous work on the nitroethylene molecule is scarce. Karle et al. discussed its unimolecular decomposition using MP2, MP4 and G2 methods[4] and Zhang and co-workers focused on ground-state isomerization reactions and vertical calculations of the first five electronic transitions, respectively at the DFT/B3LYP/6-31G* and TD-DFT-B3LYP/6-31G* levels of theory.[23] Shamov and Khrapkovskii considered the pyrolysis mechanism of nitroethylene using the B3LYP/6-31G(d) method.[24] Khrapkovskii and co-workers reviewed quantum chemical data on gas-phase decomposition mechanisms of C-nitro compounds including nitroethylene.[25]

Concerning the excited electronic states of nitroethylene up to the year 2006, apparently only three other theoretical studies and an older experimental work can be found in the literature. The spectrum of nitroethylene in gas phase was measured in the 1960s by Loos and co-workers,[26] who observed a very weak band at 4.2 eV and an intense band centered at 6.12 eV with a shoulder at 5.12 eV. Those authors used the semiempirical Pariser−Parr−Pople configuration interaction (PPP-CI) method to assign the intense band and its shoulder to $\pi-\pi^*$ transitions. In another work, Ha employed SCF-CI wave functions and a small Gaussian basis set to find also the character of the first band as a n-π^* transition and of the intense band and its shoulder as two $\pi-\pi^*$ transitions.[27] In 2006, Zhang and co-workers[23] examined vertical excitations computed at the TDDFT-B3LYP/6-31G* level once more confirming the $\pi-\pi^*$ character of the intense band and its shoulder.

Recently, we carried out a systematic examination of the electronic spectrum of nitroethylene using a variety of methods:[28] the approximate coupled-cluster singles and doubles wave function with the resolution of the identity (RI-CC2), the time dependent density functional theory with the CAMB3LYP functional (TDDFT/CAMB3LYP) and the DFT multireference configuration interaction (DFT/MRCI). Vertical transition energies and optical oscillator strengths of up to 20 singlet transitions were computed. Additionally, semiclassical simulations of ultraviolet (UV) spectra at the RI-CC2 and DFT/MRCI levels were performed. The main features in the UV spectrum were assigned to a weak n-π^* transition, and to two higher energetic ones as $\pi-\pi^*$ bands. The simulated spectra is in good agreement with the experimental spectrum. These features of the nitroethylene spectrum are similar in molecules containing NO_2 groups. The transition energies of the bands in the DFT/MRCI simulation agreed quite well with experiment, although it overestimated the band intensities. The RI-CC2 calculation produced intensities comparable to the experiment, but the bands were blue-shifted by 0.5 eV. A strong $\pi-\pi^*$ band, not previously measured, was found in the 8−9 eV range.

The goal of this work is to discuss the photochemical pathways for the decay of nitroethylene to the ground state. In this discussion, the photodynamics of ethylene[29−35] and fluoroethylene[36] will guide us, the latter serving as an example for a polar biradicoloid. Both cases can be qualitatively explored by a 3 × 3 CI analytical model as developed by Bonačić-Koutecký and Michl.[37,38] This model predicts for non-symmetric biradicaloids like fluoroethylene the appearance of a degeneracy between the S_0 and S_1 states by simple torsion of the CC double bond, as was confirmed by quantum chemical calculations.[36] In contrast, it is well documented that in ethylene the torsion is not sufficient for reaching an intersection with the ground state but that pyramidalization and hydrogen transfer modes play an important role.[29,31,32] From this point of view, nitroethylene is an interesting example, since it polarizes the C═C bond due to electronegativity differences of the groups bonded to it, but it also includes contributions from π conjugation and lone pair orbitals. For this reason, a multitude of excited states already appears in the case of vertical excitations,[28] and conical intersections should involve CH_2 and NO_2 torsions. The calculation of excited-state energy surfaces and the search for conical intersections of nitroethylene is thus even more involved.

In this work, we employ the multireference configuration interaction with singles and doubles (MR-CISD) method[39] to calculate potential energy curves for selected coordinates, to determine minima on the crossing seam (MXS) and to characterize nonadiabatic interactions between different electronic states of nitroethylene. These features should allow us to develop an overall picture of the nitroethylene photochemistry through possible nonradiative decay mechanisms originating in a bright electronically excited molecule leading it to reach the ground state.

2. COMPUTATIONAL DETAILS

The calculations were carried out in two steps. The first one consisted of a state-averaged multiconfiguration self-consistent field (SA-MCSCF) calculation followed by a multireference configuration interaction with single and doubles excitations (MR-CISD). The state averaging was performed with equal weights and included six states (SA-6), namely, the ground state S_0 ($1^1A'$), three A″ and two A′ states in the case of vertical excitations. For describing these excitations, a complete active space—CAS(8,6)—including eight electrons and six orbitals, the four highest occupied orbitals (two a″ and two a′), and two virtual orbitals of a″ symmetry, was chosen. The SA-MCSCF character of the orbitals are 2a″ [π (NO_2)], 15a′ [nσ], 16a′ [nσ(O)], 3a″ [π (C═C+ NO_2)], 4a″ [π^*] and 5a″ [π^*] (see Figure 1). The 15a′ and 16a′ orbitals are respectively n_+ and n_- type-orbitals because the former corresponds to symmetric linear combinations of the oxygen lone pair orbital and the latter, the highest occupied molecular orbital (HOMO), represents the antisymmetric combination.[28] This SA-6-CASSCF calculation was followed by a MR-CISD with the reference configurations generated from the same CAS (8,6)

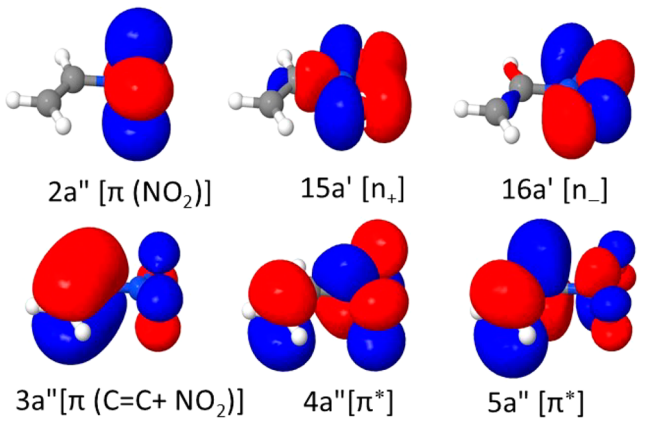

Figure 1. SA-MCSCF active space nitroethylene molecular orbitals.

dx.doi.org/10.1021/jp507396e | J. Phys. Chem. A 2014, 118, 12011−12020

Table 1. Computed MCSCF, MR-CISD, and MR-CISD+Q Vertical Excitation Energies ΔE (eV) in Comparison with Previous Results and Experimental (Exp.) Data[a]

state	MCSCF	MRCI	MRCI+Q	f	character	DFT/MRCI[b]	exp.
S_1-$1^1A''$	3.47	3.69	4.03	0.000	$n_-\rightarrow\pi^*$ (16a′→4a″)	3.62(0.000)	4.20(0.002)
S_2-$2^1A''$	4.06	4.14	4.48	0.000	$n_+\rightarrow\pi^*$ (15a′→4a″)	4.11(0.000)	
S_3-$2^1A'$	6.08	6.33	6.05	0.034	$\pi\rightarrow\pi^*$ (2a″→4a″)	5.19(0.051)	5.12(0.012)
S_4-$3^1A''$	7.00	7.33	7.37	0.000	$n_+\rightarrow\pi^*$ (15a′→5a″)	6.25(0.000)	
S_5-$3^1A'$	7.18	7.58	6.00	0.375	$\pi\rightarrow\pi^*$ (2a″→4a″)	6.09(0.432)	6.12(0.304)

[a]The computed MR-CISD oscillator strengths (f) are also reported. The DFT/MRCI and experimental oscillator strength values are shown in parentheses. [b]Our previous results.[18] [c]Experimental data.[12]

space and applying the interacting space restriction.[40] This orbital space has been chosen to represent the reference space for the computation of the five lowest singlet valence excited states as discussed in our previous work.[28] Since the focus of this work is laid on the exploration of the photodeactivation mechanism of the valence states, Rydberg states, which appear above those in the upper range of the states chosen,[28] were not included in our calculations.

The carbon, oxygen, and nitrogen 1s orbitals were frozen in the CI calculations. The Davidson[41,42] corrections for size-extensivity were also computed. The 6-31++G** Gaussian basis set[43] was used. This type of calculation is the standard one and will be denoted MRCI. It will be used for the calculation of the vertical spectra, potential curves, and MXS structures. Two significantly extended approaches will be described in the following paragraph. They will be used only for calculating vertical excitation energies.

For vertical excitations, two additional kinds of calculations were carried out. In the first, the basis set was extended significantly to 6-311+G(2d1f)[44,45] on the heavy atoms. For the hydrogen atoms, a 6-31G** basis was chosen. The reference space was kept at the CAS(8,6) level. This calculation is denoted MRCI(extbas). In the second kind of calculation, the active space of the reference wave function was increased while keeping the basis set at the 6-31++G** level. This extended reference wave function is denoted RAS(2,1)CAS(8,6)AUX-(2,1). The acronym RAS stands for a restricted active space and AUX for auxiliary space. The notation RAS(2,1) means that two a′ and one a″ orbital were moved from the doubly occupied space into the active space. In the case of AUX(2,1), two a′ and one a″ virtual orbitals were moved into the active space. The CAS(8,6) remained unchanged. Only single excitations were allowed from the RAS and into the AUX space. This configuration space was used as a wave function in the MCSCF calculation and as a reference wave function in the case of the MR-CISD calculation. The corresponding calculation is named MRCI(extref).

The geometries were described by natural internal coordinates[46] and optimized using the direct inversion in the interactive subspace (GDIIS) method.[47] Geometry optimizations and determination of the minima on the crossing seam (MXS), i.e., the conical intersections respectively employed analytic MR-CISD gradients[48,49] and analytic MR-CISD nonadiabatic coupling vectors.[50−52] The exception was the S_2/S_1 and S_5/S_4 conical intersections, which were converged only at the CAS (8,6) level; in these cases, a single-point MR-CISD with the same type of wave function used for the other geometries were done. The potential energy curves were obtained with full optimization of all coordinates except the selected coordinate for constructing the potential curve.

The COLUMBUS suite of programs was used for all calculations.[53−55] The calculations were in part performed using the parallel version of COLUMBUS.[56,57] The atomic orbital (AO) and the derivative integrals were calculated using the DALTON program.[58]

3. RESULTS AND DISCUSSION

3.1. Vertical Transitions. The DFT/B3LYP//6-311G+(2df,2p) planar ground state geometry obtained in our previous work[28] was employed for the vertical calculations. Transition energies and oscillator strengths from the S_0 ground state to the S_1−S_5 valence excited states were computed. The results are collected in Table 1 together with our previous DFT/MRCI results[28] and available experimental data. The SA-6-CASSCF(8,6) molecular orbitals are depicted in Figure 1. The results of the two additional vertical calculations are shown in Table 2.

Table 2. Computed MCSCF, MR-CISD, and MR-CISD+Q Vertical Excitation Energies ΔE (eV) Using the MRCI(extbas) and MRCI(extref) Approaches

state	MCSCF (extbas)	MRCI (extbas)[a]	MRCI +Q (extbas)[a]	MCSCF (extref)	MRCI (extref)[b]	MRCI +Q (extref)[b]
S_1-$1^1A''$	3.45	3.86	4.00	3.64	3.94	4.07
S_2-$2^1A''$	4.03	4.39	4.47	4.53	4.48	4.40
S_3-$2^1A'$	6.07	6.30	6.10	6.34	6.09	5.74
S_4-$3^1A''$	6.98	7.62	7.28	7.13	7.39	7.38
S_5-$3^1A'$	7.12	7.23	6.15	8.18	7.34	5.83

[a]6-311+G(2d1f)/ 6-31G**// CAS(8,6)-MR-CISD. [b]6-31++G**// RAS(2,1)CAS(8,6)AUX(2,1)-MR-CISD.

The measured weak band is assigned to the two $n\rightarrow\pi^*$ transitions involving states S_1 and S_2. The MR-CISD transition energies computed in this work for the S_1 and S_2 transitions are (MR-CISD+Q values between parentheses): 3.69 eV (4.03 eV) and 4.14 eV (4.48 eV). These two dark transitions are respectively excitations from the n_- (16a′) and n_+ (15a′) orbitals localized on the NO_2 moiety to the same π^* (4a″) final orbital. There is another dark transition (S_4) that also originates from the n_+ (15a′) orbital, but in this case is an excitation to the higher π^* (5a″) orbital.

The S_5 state corresponds to the measured band maximum and the S_3 corresponds to the band shoulder; both transitions are of $\pi\rightarrow\pi^*$ type. The S_3 state has MR-CISD transition energies (MR-CISD+Q between parentheses) of 6.33 eV (6.05 eV) and oscillator strength f = 0.034 (MR-CISD) and the S_5

dx.doi.org/10.1021/jp507396e | J. Phys. Chem. A 2014, 118, 12011−12020

has 7.58 eV (6.00 eV) and $f = 0.375$. The S_3 state is a transition from a π (2a″) orbital localized on the NO_2 group to a π^* (4a″) orbital while the S_5 state, the brightest of the computed set, is an excitation from the π (3a″) orbital to the π^* (4a″) having contributions from electron density distributed over the CC bond as well. As it is typical of energetic molecules, the bright $\pi-\pi^*$ transition involve orbitals mostly localized on the NO_2 moiety.

The transition energy of the S_5 bright $\pi-\pi^*$ transition computed at the MR-CISD+Q level agrees quite well with the experimental band maximum. The corresponding MR-CISD value is too high in energy. The weaker $\pi-\pi^*$ transition (S_3) is too high at both the MR-CISD and MR-CISD +Q levels.

In contrast to our previous results,[28] there is an inversion of the MR-CISD energy ordering of the $n-\pi^*$ (S_4) and $\pi-\pi^*$ (S_5) transitions in comparison with the DFT/MRCI calculations (Table 1). However, the vertical energy ordering becomes compatible with DFT/MRCI after inclusion of the Davidson (MR-CISD-Q) correction.

An overall comparison of the MCSCF transition energies with all the available MR-CISD values (Table 1 and Table 2) shows relatively little changes except for the MCSCF(extref) results of the S_5-$3^1A'$ state. This shows that our standard CAS(8,6) reference space is in principle flexible enough to represent the major features of all states investigated except the one mentioned. In this case, the MCSCF(extref) enhances the weight of $\pi-\pi^*$ excitations on the cost of artificial $n^2-\pi^2$ excitations; thus, the character of the S_5 state is considerable improved in spite of the higher MCSCF excitation energy. The MR-CISD approach actually increases in most cases the excited state energies relative to the ground state; the most prominent exception is the S_5 state for which the MRCI(extref) not only enhances the weight of the excitation from the π (3a″) to the π^* (4a″) orbital, but also stabilizes this state relative to the others. Significant changes are observed by applying the Davidson correction which decreases the excitation energies of the two $\pi-\pi^*$ states $2^1A'$ and $3^1A'$ considerably, especially of the latter state. The energetic location of both states is especially improved by extension of the active space to the extref case, but the $2^1A'$ state is still about 0.6 eV above the experimental value. Further extension of the active space beyond the present RAS/CAS/AUX scheme of 14 electrons in 12 active orbitals would be necessary in order to increase especially the stability of the $2^1A'$ state, but such an approach will render the calculations very costly. Since our focus was not so much concentrated on the vertical excitations but on the exploration of the photodynamical deactivation picture, we did not follow this path further.

Overall, the MR-CISD and MR-CISD+Q methods provide a good starting point for the following discussion of reaction paths on excited-state energy surfaces and the determination of conical intersections. These investigations will lead into regions of the energy surfaces far away from the Franck−Condon region, and it is this aspect where the multireference method will be most useful. For this purpose, we have chosen the standard MRCI/CAS(8,6) approach which gives a good balance between computational efficiency and flexibility of the wave function.

3.2. Potential Curves. Following the experience with the photodeactivation mechanisms found for ethylene[31] and fluoroethylene,[36] the MR-CISD potential energy curves of the states S_0-S_5 were calculated for two rigid torsions: of the NO_2 group around the C−N bond (Figure 2) and of the CH_2 group around the C═C bond (Figure 3); the latter torsion also occurs in ethylene.[31] The MR-CISD CH_2 out-of-plane bending

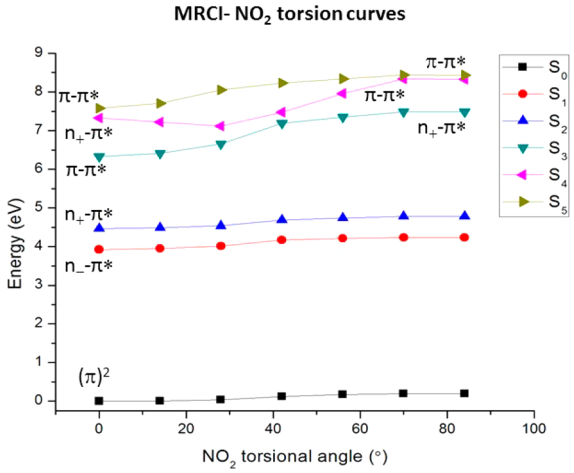

Figure 2. Rigid MR-CISD potential energy curves for NO_2 rotation around the CN bond starting from the DFT/B3LYP//6-311G +(2df,2p) ground state geometry.

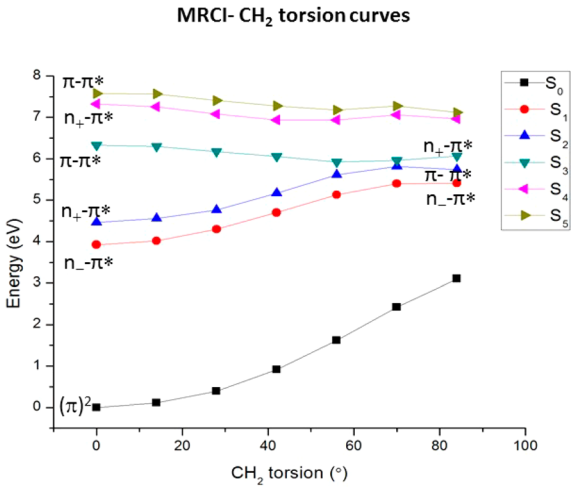

Figure 3. Rigid MR-CISD potential energy curves for CH_2 rotation around the CC bond starting from the DFT/B3LYP//6-311G +(2df,2p) ground state geometry.

curves (Figure 4) were also computed. In all cases, the calculations started from the DFT/B3LYP//6-311G+(2df,2p) ground state geometry.[28]

We have seen above that the $\pi-\pi^*$ S_3 state ($2^1A'$) is a vertical transition characterized by molecular orbitals mostly localized in the NO_2 moiety. Upon NO_2 torsion, the S_3 excited state is destabilized by about 0.5 eV (Figure 2). The other states are destabilized also, albeit to a lesser degree. A partial exception to this behavior is the S_4 state that, after initially stabilizing, destabilizes also following the behavior of the other states. There is an avoided crossing between S_3 and S_4 at around 45° where the character of the two states is exchanged. S_4 now acquires $\pi-\pi^*$ character and S_3 becomes $n_+-\pi^*$. For greater torsion angles, the S_4 and S_5 states become almost degenerate. The small gap in the curves between the pair of states S_3-S_4 and S_4-S_5 indicates the possible presence of conical intersections and crossing seams involving torsion of

dx.doi.org/10.1021/jp507396e | J. Phys. Chem. A 2014, 118, 12011−12020

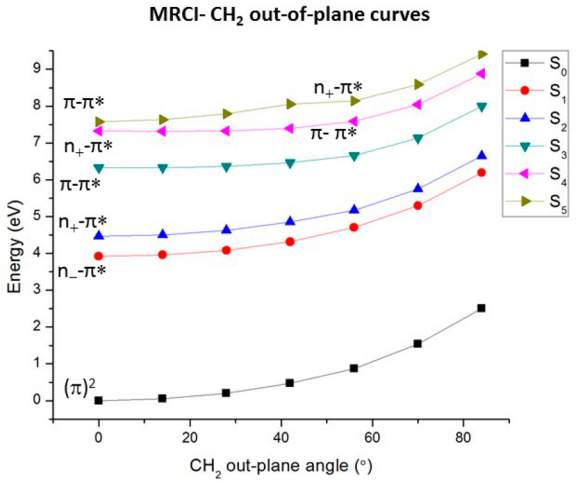

Figure 4. MR-CISD CH_2 out-of-plane bending starting at the DFT/B3LYP//6-311G+(2df,2p) ground state geometry.

the NO_2 moiety. In fact, these conical intersections were found (see below).

For the CH_2 torsion curves (Figure 3), the picture has more features. The S_3 state in nitroethylene, a $\pi-\pi^*$ vertical excitation, is stabilized by about 0.5 eV for increasing CH_2 torsion angles. The S_2 and S_3 states reveal an avoided crossing and exchange their character at an angle of about 56°. From this angle onward, the dominant character of S_3 is $n_+-\pi^*$ while the S_2 state becomes $\pi-\pi^*$. Both states become almost degenerate at 70° with an energy difference of 0.3 eV, thus indicating a crossing.

Similar to ethylene, the ground state S_0 ($1^1A'$) in nitroethylene destabilizes strongly upon CH_2 torsion (Figure 3) by almost 3 eV. This situation leads to a reduction of the gap to the first excited state (S_1) by about 2 eV, a 50% decrease. This contrasts with the very small destabilization of the ground state upon NO_2 torsion (Figure 2). For a CH_2 torsion angle of ~70°, the character of the S_0 state, π^2 at 0°, now has a $\pi-\pi^*$ configuration that contributes with a weight of about 20%. For CH_2 torsion angles of 90°, the S_0 state is dominated by a $\pi-\pi^*$ configuration with weight of 57%, while for S_1 another $\pi-\pi^*$ configuration (weight = 12%) mixes with the dominant $n_--\pi^*$ character (weight = 36%). This character is essentially maintained in the MXS (S_1/S_0) found (see Table 3).

For ethylene, it has been shown that pyramidalization of the CH_2 group (combined with partial hydrogen migration) is important for reaching the conical intersection between a $\pi-\pi^*$ state and the S_0.[29,31,59−61] Therefore, we also investigated the effect of the CH_2 out-of-plane bending (i.e., pyramidalization) coordinate through the potential energy curves of nitroethylene.

The MR-CISD CH_2 out-of-plane bending curves of nitroethylene starting from the ground state geometry are shown in Figure 4. Overall, the six states including the ground state steadily destabilize by about 1 eV. The S_4 and S_5 exchange $n_+-\pi^*$ and $\pi-\pi^*$ character via an avoided crossing for a CH_2 out-of-plane angle of 55°. The energies of the pair of S_4/S_5 curves slightly decreases with increasing CH_2 out-of-plane angle, and the energy splitting remains very small. Thus, for nitroethylene there is no significant effect of the CH_2 out-of-plane motion on the expected conical intersection structures.

3.3. Ground State and Structure of the Conical Intersections. The SA-6-MCSCF/MR-CISD optimized geometries of the ground state and of the minima on the crossing seam (MXS) are shown in Figures 5−8. The optimized ground state distances and angles computed in this work at MR-CISD level are displayed in Figure 5a. They agree very well with the ones obtained previously by means of the DFT/B3LYP approach.[28]

The main feature of the MXS (S_1/S_0) (Figure 5b) as compared with the MR-CISD ground state is the position of the CH_2 group, twisted by 97°: it is now essentially perpendicular to the original molecular plane. There is a CC bond elongation of 0.14 Å and also an elongation of the NO bonds: the larger NO elongation is 0.14 Å, and the smaller one

Table 3. MR-CISD Character of the Conical Intersections with Corresponding Coefficients

MXS	character
S_1/S_0	$(0.72)n_+-\pi^* + (0.47)\pi-\pi^*/(0.85)n_-\pi + (0.17)\ n_-^2-\pi^*\pi^* + (0.16)\ (\pi^*)^{2a}$
S_2/S_1	$(0.79)n_+-\pi^* + (0.27)\pi-\pi^*/(0.83)n_-\pi^* + (0.29)(\pi^*)^2$
S_3/S_2	$(0.38)n_-\pi^* + (0.30)\ \pi^2-(\pi^*)^2 + (0.29)\ \pi-\pi^*/\ (0.46)\ n_-\pi^* + (0.28)\ n_+-\pi^*$
S_4/S_3	$n_-\pi-\pi^*\pi^*/(0.64)\pi-\pi^* + (0.29)\ n_-\pi^{*b}$
S_5/S_4	$(0.54)(n_-)^2-(\pi^*)^2 + (0.42)\ \pi^2-(\pi^*)^2/(0.47)n_+-\pi^* + (0.35)\ n_-\pi-\pi^*\pi^{*c}$

[a] S_0: double excitation from n_ to the two distinct virtual π^* orbitals. [b] S_4: double excitation from n_ and π to the two distinct virtual π^* orbitals. [c] S_5: double excitation from n_ to a π^*.

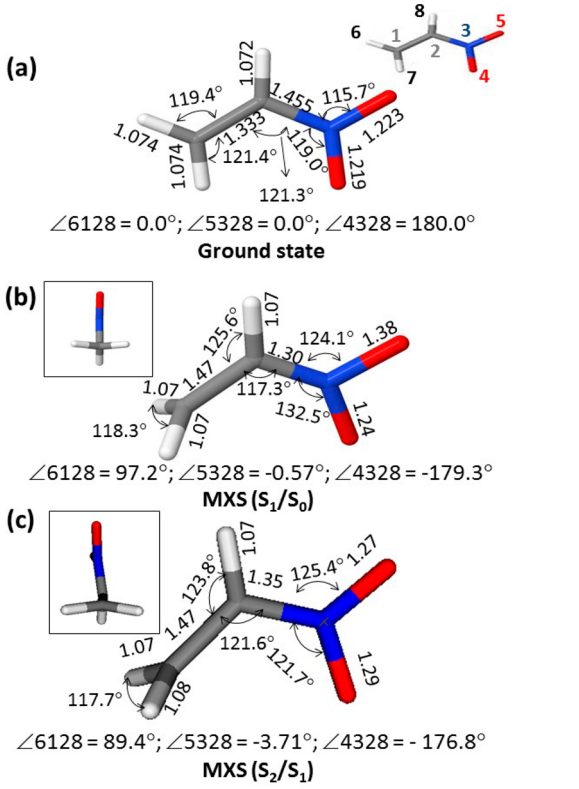

Figure 5. Optimized geometries of nitroethylene. (a) MR-CISD ground state. Computed conical intersections (MXS): (b) MR-CISD MXS (S_1/S_0), and (c) CASSCF MXS (S_2/S_1). Angles are in degrees and distances are in Å. The dihedral angles are shown according to the numbering given in the inset at panel a. Insets of panels b and c are front views of the corresponding structures.

dx.doi.org/10.1021/jp507396e | J. Phys. Chem. A 2014, 118, 12011−12020

is 0.02 Å. In contrast, the C−N bond shortens by −0.16 Å. Although the torsional structure of the MXS (S_1/S_0) could be deduced from the large CH_2 torsion angle of the corresponding potential curves, Figure 3, the just indicated additional bond length variations are crucial to reach the conical intersection. As already mentioned above, out-of-plane bending of the CH_2 group is not important in nitroethylene.

The MXS (S_2/S_1) (Figure 5c) is overall similar to the MXS (S_1/S_0) (Figure 5b); the torsion of the CH_2 group by about 90° is also the prominent feature. There are differences in the elongation of the NO and CN bonds of the MXS (S_2/S_1) as compared to the MXS (S_1/S_0) as well as differences in the angular values despite the two insets looking very similar.

The MXS (S_3/S_2) (Figure 6a) has distinct features. There is a torsion of the NO_2 group and of the C_2H_8 bond (for atomic numbering, see the inset of Figure 5a) in the opposite sense leading to an almost perpendicular orientation of both relative to the ground state molecular plane (see inset of Figure 6a). There is an opening of the ONO bond and a visible pyramidalization of the NO_2 group. The CN distance in the MXS (S_3/S_2) structure decreases by 0.03 Å as compared to the ground state. The three CH distances decrease slightly by 0.04 Å, while the larger NO distance increases by 0.16 Å and the smaller one increases by 0.02 Å. The CN bond shortens by 0.04 Å. There are considerable variations of the valence angles, the most pronounced one being the 9° increase in the NO_2 opening angle and the CH_2 opening angle decreasing by 2.6°.

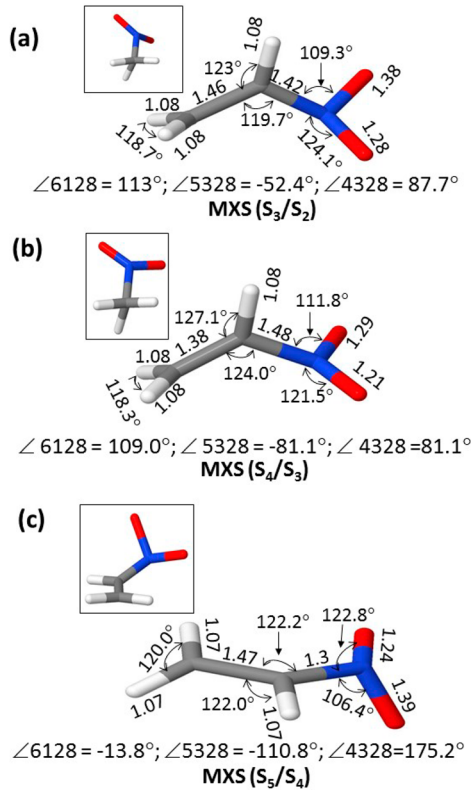

Figure 6. Computed conical intersections (MXS): (a) MR-CISD MXS (S_3/S_2), (b) MR-CISD MXS (S_4/S_3), and (c) CASSCF MXS (S_5/S_4). Angles are in degrees and distances are in Å. The dihedral angles are shown according to the numbering given in the inset in Figure 5, panel a. Insets are front views of the corresponding structures.

Although the shape of the MXS (S_4/S_3) (Figure 6b) is overall similar to the MXS (S_1/S_o) (Figure 5b) and MXS (S_2/S_1) (Figure 5c) conical intersections, there are important differences. In the following, we continue to compare distances with the ground state values. The CC bond of the MXS (S_4/S_3) (Figure 6b) elongates by 0.13 Å and the CN bond by 0.3 Å. The N_3O_5 bond stretches by 0.07 Å, while the other NO bond barely changes. In comparison with the other conical intersections, the MXS (S_4/S_3) stretches almost all bonds, and the CH_2 group twisted by about 80° as compared to the ground state structure. The NO_2 group is also twisted almost by 90° and displays some pyramidalization.

In the MXS (S_5/S_4) (Figure 6c), the structure is almost planar; the CH_2 group is twisted by a small angle as compared to the other conical intersections, but overall the geometry is more planar in comparison with the other MXS's. The NO_2 angle increases by 5.5° and all the bonds elongate, excepting the CN and CH distances.

Table 3 collects the character of the conical intersections found. It can be seen that the character of the MXS's could be qualitatively inferred from the computed potential energy curves. In particular, the overall similarities of the MXS (S_1/S_0) and MXS (S_2/S_1) geometries discussed above have correspondence with the respective character. The expected multiconfiguration character of the states in most intersections is clear, and $\pi-\pi^*$ type transitions are relevant in the five intersections. Moreover, there is an important role in the character of all conical intersections played by the lone pair (n) orbitals localized on the NO_2 moiety.

3.4. Photodynamical Mechanism. The g- and h-vectors characterizing the conical intersection[50,52,62,63] are shown in Figures 7 and 8 for the five computed MXS structures. The g-vector is defined by the energy gradient difference between the two states, and the h-vector is the nonadiabatic coupling vector. A molecular deformation along these vectors determines the branching space, lifts the degeneracy of the states, and describes possible reaction coordinates.

For the MXS (S_1/S_0), the g-vector (Figure 7a) is dominated by the CN stretching and NO_2 wagging. The h-vector represents a CH_2 torsion around the CC bond. The CC torsion leading to a reduction of the S_1/S_0 gap also occurs in ethylene and fluorethylene. As discussed before for ethylene, the S_1/S_0 gap is reached via CH_2 pyramidalization and partial hydrogen migration[31] while in fluorethylene CC torsion and stretching reduce the S_1/S_0 gap.[36] Therefore, in this case nitroethylene resembles more the fluorethylene case because for both molecules, in contrast to ethylene, the CH_2 pyramidalization does not play a role.

Although the geometry of the MXS (S_2/S_1) is similar to the MXS (S_1/S_0), their g- and h- vectors (Figure 7b) display distinct features. The most important ones are the bending deformation of the NO_2 group and the absence of CH_2 motion. Therefore, only NO_2 deformation is relevant to reach the S_2/S_1 intersection.

The MXS (S_3/S_2) g- and h- vectors (Figure 7c) display pronounced stretching modes of the NO_2 bonds, combined with an angular deformation of the NO_2 group and a stretching of the CC bond. The h-vector also indicates a CH_2 torsion and an angular deformation of the CH_2 bond. The g- and h- vectors of the MXS (S_4/S_3) (Figure 8a) are dominated by an out-of-plane deformation of the NO_2 group with a contribution of a CC stretching. The MXS (S_5/S_4) (Figure 8b) g- and h-vectors

dx.doi.org/10.1021/jp507396e | J. Phys. Chem. A 2014, 118, 12011−12020

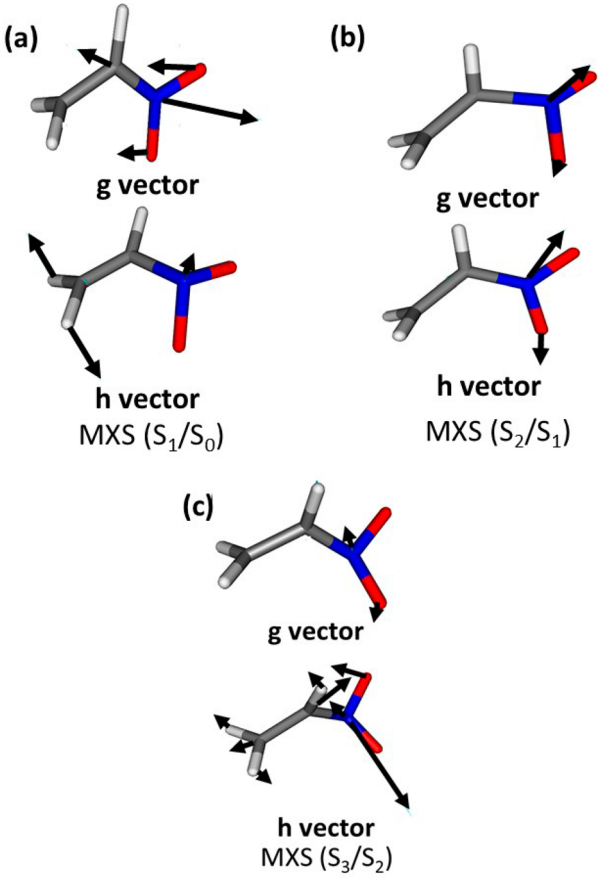

Figure 7. Computed g- and h-vectors of the conical intersections found. (a) MR-CISD MXS (S_1/S_0), (b) CASSCF MXS (S_2/S_1), and (c) MR-CISD MXS (S_3/S_2). The arrows are not to scale between different pictures.

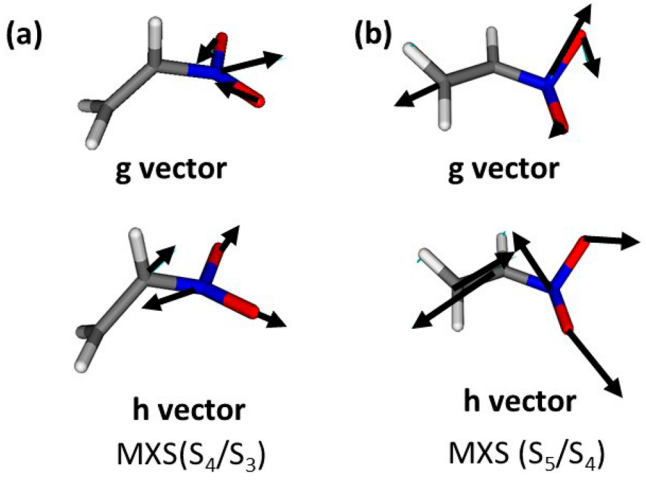

Figure 8. Computed g- and h-vectors of the conical intersections found. (a) MR-CISD MXS (S_4/S_3) and (b) CASSCF MXS (S_5/S_4). The arrows are not to scale between different pictures.

also display a deformation of the NO_2 group and CC stretching, similarly to the other conical intersections.

The existence of a series of conical intersections in nitroethylene suggests nonradiative deactivation processes via internal conversion (IC). In Figure 9, an overview of possible deactivation paths based on the energies and geometries of the conical intersections is presented. It can be seen that the S_5/S_4,

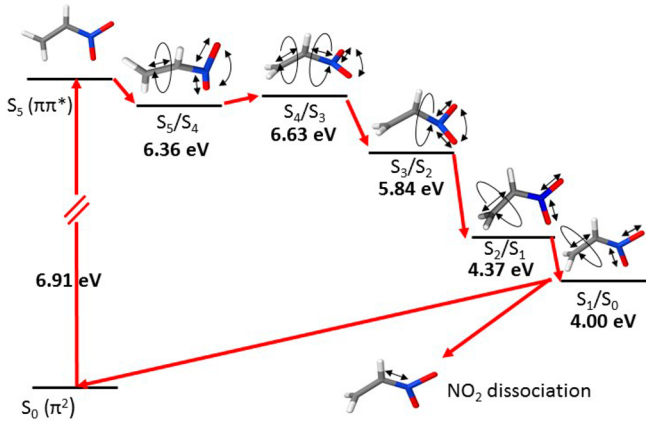

Figure 9. Proposed photochemical nonradiative deactivation process. The path leading to the possible release of NO_2 is also indicated. The main structural modifications of the conical intersections with respect to the ground state geometry are displayed.

S_4/S_3 and the S_3/S_2 conical intersections are quite close in energy. Based on this scheme and along with the computed potential energy curves, the following nitroethylene deactivation photodynamic process can be deduced.

Bearing in mind that because nitroethylene is a multistate problem, the dynamics need not proceed necessarily through minimum-energy conical intersections, but may take shortcuts through near-degeneracies of higher energy (e.g., as observed in the ethylene dynamics[34]), we suggest the following photodynamic mechanism. The photodynamics starts from the Franck−Condon region by populating the bright S_5 state. The torsion around the CC bond (Figure 3) does not lead to a pronounced stabilization as is found in ethylene[31] or fluoroethylene.[36] Therefore, this torsion alone does not lead to a region of intersection with the S_4 state. The NO_2 torsion (Figure 2), however, points to an S_5/S_4 intersection at a relatively small torsion angle. The internal conversion to the S_4 state occurs mostly by CC stretching and NO_2 torsion (MXS (S_5/S_4) - see Figure 6c and Figure 8b), with contribution of CH_2 twisting. The CC bond lengthens from the ground state value of 1.33 Å to 1.47 Å and the CN bond shortens from 1.46 to1.37 Å. The energy of this MXS is stabilized by 0.4 eV as compared to the vertical excitation. To continue to the S_4/S_3 conical intersection (Figure 6b) requires significant torsions around the CH_2 and NO_2 groups (Figure 8a). In the MXS (S_4/S_3) structure the C_2H_8 bond is now almost perpendicular to the planes of the CH_2 and NO_2 groups, with the CC and CN bond lengths decreasing and increasing, respectively, as compared to the MXS (S_5/S_4). The computed potential curves confirm this picture: upon NO_2 (Figure 2) and CH_2 (Figure 3) torsion, the S_4 state slightly stabilizes. The MXS (S_4/S_3) is only 0.14 eV higher in energy than the MXS (S_5/S_4) and certainly accessible energetically within the deactivation dynamics. The S_3 state is also a bright state. Thus, it can be also populated directly through an excitation from the ground state even though with a smaller probability as compared to the S_5 state. The CH_2 torsion stabilizes the S_3 state and leads to an intersection with S_2. On the other hand, NO_2 torsion destabilizes S_3. These features are reflected in the structure of the MXS (S_3/S_2) (Figure 6a) where a rotation of the NO_2 group with respect to the MXS (S_4/S_3) is observed. Moreover, the CC bond is stretched in comparison with the latter MXS. The MXS (S_3/S_2)

dx.doi.org/10.1021/jp507396e | J. Phys. Chem. A 2014, 118, 12011−12020

undergoes a significant energetic stabilization by 0.8 eV as compared to the MXS (S_4/S_3).

The energies of the S_1 and S_2 states upon CH_2 torsion are energetically close in the whole range (Figure 3), particularly at the 90 °CH_2 torsion angle, a torsional region that is also assumed by the preceding MXS (S_3/S_2). In fact, the MXS (S_2/S_1) is characterized by a CH_2 torsion of ∼90° (Figure 5c), though the NO_2 bending (see Figure 7c), combined with a relevant shortening of the CC bond and elongation of the CN and NO bonds, led to the S_1/S_0 intersection (Figure 7a).

The MXS (S_1/S_0) is characterized by a CH_2 torsion of ∼90° similarly to the MXS (S_2/S_1). As was already noted above, this intersection is not only achieved by this torsion but also by non-negligible changes of the CC, CN, and NO bond distances with respect to the ground state values suggestive of hot ground state dynamics after transition to S_0. The energy of the MXS (S_1/S_0) is stabilized by ∼0.4 eV in relation to the MXS (S_2/S_1).

In view of the 3 × 3 CI analytical model as developed by Bonačić-Koutecký and Michl,[37,38] the torsion of the CH_2 in nitroethylene from the planar geometry (Figure 3) reduces the S_1/S_0 gap as seen in the corresponding potential curves. A NO_2 torsion has little influence on the S_1/S_0 gap (Figure 2). This reduction according to that theory is due to an increased electronegativity difference of the CC bond upon CH_2 torsion. However, this gap reduction in nitroethylene is not as pronounced as, e.g., in fluoroethylene. In the latter,[36] a rigid CC torsion reduces the gap to ∼1 eV. In contrast, in nitroethylene a rigid CC torsion leads to a gap of ∼2 eV and in ethylene to ∼2.3 eV. However, as said above, a combination of bond changes, namely, a significant lengthening of the CC (0.15 Å) and one NO bond (N_3O_5 = 0.14 Å), and also a shortening of the CN bond (−0.16 Å), as compared to the ground state geometry, takes place and is responsible for reaching the S_1/S_0 intersection. Moreover, the energy gradient difference g-vector of the MXS S_1/S_0 (Figure 7a) indicates possible NO_2 release through activation of the CN bond stretching. No pyramidalization of the CH_2 or NO_2 groups is observed. In this sense, the situation in nitroethylene can be considered similar to the polar fluoroethylene, with a significantly larger contribution of changes in the bond distances as compared to the ground state.

After a nonadiabatic transition, the vibrational energy acquired in the process by the molecule concentrates in the small number of vibrational modes that define the conical intersection.[64] Nitro compounds are usually thermally unstable and composed of easily broken covalent bonds such as N−N, O−C, and C−N. Release of the very labile NO_2 group in these molecules is thus rather probable in the hot ground state dynamics. The g-vector in the MXS (S_0/S_1) (Figure 7a), as discussed above, indicates the activation of a CN stretching mode. Therefore, it is expected that upon nonradiative transitions these modes might favor the release of the NO_2 group.

4. CONCLUSIONS

Extensive MR-CISD calculations were performed to study photodeactivation mechanisms of nitroethylene involving the first five valence excited states. Calculations of vertical excitations were carried out first. These calculations presented good agreement with our previous calculations and the experimental spectrum, excepting an inversion of the energy ordering of the last two transitions, the n−π^* (S_4) and π−π^* (S_5).

The potential curves for torsion and pyramidalization of the CH_2 group and the torsion of the NO_2 moieties were computed. Five conical intersections, one between every pair of adjacent states, were found: S_5/S_4, S_4/S_3, S_3/S_2, S_2/S_1, and S_1/S_0.

The computed g- and h-vectors describing the shape of the intersection cone point to an important role played by the torsions of the CH_2 and NO_2 groups, with contributions of other modes such as CC and CN stretching. Similarities between the behavior of nitroethylene and previous work on the ethylene[31] and fluorethyelene[36] molecules were explored.

From the computed potential energies and the conical intersections found, a photochemical mechanism of nitroethylene deactivation could be proposed starting in the bright S_5 (π−π^*) excited state. After a Franck−Condon excitation to this state, a nonradiative chain of deactivation processes of nitroethylene from this state downward can proceed through conical intersections mostly characterized by twisting the CH_2, with important contributions from deformations of the NO_2 group and CC and CN bond stretches. Furthermore, the modes of the MXS (S_1/S_0) g-vector indicate the possibility of NO_2 release in the ground state, an important process in nitro molecules with explosive properties.

The results of this work have shed light on the photochemistry of nitroethylene, in particular on the importance and role of the conical intersections between adjacent pair of states. Moreover, these results will allow further chemical dynamics investigations on this molecule.

■ ASSOCIATED CONTENT

Supporting Information

MR-CISD absolute energies and the Cartesian coordinates of the conical intersections. This material is available free of charge via the Internet at http://pubs.acs.org.

■ AUTHOR INFORMATION

Corresponding Authors

*E-mail: itamar@ime.eb.br.

*E-mail: hans.lischka@univie.ac.at.

Notes

The authors declare no competing financial interest.

■ ACKNOWLEDGMENTS

I.B. thanks the Brazilian Agencies CNPq, Faperj and CAPES, and the Brazilian Army, for support of this work. H.L. and I.B. acknowledge support from Capes in the framework of the Science without Borders Brazilian Program. H.L. is "Bolsista CAPES/Brasil". This material is based upon work supported by the National Science Foundation under Project No. CHE-1213263 and by the Austrian Science Fund within the framework of the Special Research Program F41. Computer time at the Vienna Scientific Cluster (Project Nos. 70019 and 70376) is gratefully acknowledged. Support was also provided by the Robert A. Welch Foundation under Grant No. D-0005.

■ REFERENCES

(1) Zeman, S. Sensitivities of high energy compounds. In *High Energy Density Materials*; Springer-Verlag Berlin: Berlin, 2007; Vol. *125*, pp 195−271.

(2) Attina, M.; Cacace, F.; Ciliberto, E.; Depetris, G.; Grandinetti, F.; Pepi, F.; Ricci, A. Gas-phase ion chemistry of nitramide - A mass-spectrometric and ab-initio study of H_{2n}−NO_2 and the H_{2n}−NO_2

radical$^+$, $[H_{2n}{-}NO_2]H^+$, and $[HN{-}NO2]^-$ ions. *J. Am. Chem. Soc.* **1993**, *115* (26), 12398−12404.
(3) Dewar, M. J. S.; Ritchie, J. P.; Alster, J. Ground-state of molecules 0.65. Thermolysis of molecules containing NO_2 groups. *J. Org. Chem.* **1985**, *50* (7), 1031−1036.
(4) Gindulyte, A.; Massa, L.; Huang, L. L.; Karle, J. Ab initio study of unimolecular decomposition of nitroethylene. *J. Phys. Chem. A* **1999**, *103* (50), 11040−11044.
(5) Harris, L. E. Lower electronic states of nitrite and nitrate ion, nitromethane, nitramide, nitric-acid, and nitrate esters. *J. Chem. Phys.* **1973**, *58* (12), 5615−5626.
(6) Bernstein, E. R. Role of Excited Electronic States in the Decomposition of Energetic Materials. In *Overviews of Recent Research on Energetic Materials*; Shaw, R. W.; Brill, T. B.; Thompson, D. L., Eds.; World Scientific: Singapore, 2005; Vol. *16*, p 161.
(7) Ali, A. N.; Son, S. F.; Asay, B. W.; Sander, R. K. Importance of the gas phase role to the prediction of energetic material behavior: An experimental study. *J. Appl. Phys.* **2005**, *97* (6), 7.
(8) Williams, F. Electronic states of solid explosives and their probable role in detonations. In *Advances in Chemical Physics*; John Wiley & Sons, Inc.: 1971; pp 289−302.
(9) Windawi, H. M.; Varma, S. P.; Cooper, C. B.; Williams, F. Analysis of lead azide thin-films by Rutherford backscattering. *J. Appl. Phys.* **1976**, *47* (8), 3418−3420.
(10) Sharma, J.; Beard, B. C.; Chaykovsky, M. Correlation of impact sensitivity with electronic levels and structure of molecules. *J. Phys. Chem.* **1991**, *95* (3), 1209−1213.
(11) Gilman, J. J. Chemical-reactions at detonation fronts in solids. *Philos. Mag. B: Phys. Condens. Matter Stat. Mech. Electron. Opt. Magn. Prop.* **1995**, *71* (6), 1057−1068.
(12) Kuklja, M. M.; Aduev, B. P.; Aluker, E. D.; Krasheninin, V. I.; Krechetov, A. G.; Mitrofanov, A. Y. Role of electronic excitations in explosive decomposition of solids. *J. Appl. Phys.* **2001**, *89* (7), 4156−4166.
(13) Plasser, F.; Barbatti, M.; Aquino, A. J. A.; Lischka, H. Electronically excited states and photodynamics: a continuing challenge. *Theor. Chem. Acc.* **2012**, *131* (1), 1073.
(14) Domcke, W.; Yarkony, D. R. Role of Conical Intersections in Molecular Spectroscopy and Photoinduced Chemical Dynamics. *Ann. Rev. Phys. Chem.* **2012**, *63*, 325−352.
(15) Bhattacharya, A.; Guo, Y. Q.; Bernstein, E. R. Nonadiabatic Reaction of Energetic Molecules. *Acc. Chem. Res.* **2010**, *43* (12), 1476−1485.
(16) Bhattacharya, A.; Bernstein, E. R. Nonadiabatic Decomposition of Gas-Phase RDX through Conical Intersections: An ONIOM-CASSCF Study. *J. Phys. Chem. A* **2011**, *115* (17), 4135−4147.
(17) Bernstein, E. R. Chapter Two - On the Release of Stored Energy from Energetic Materials. In *Adv. Quantum Chem.*, John, R. S., Ed.; Academic Press: 2014; Vol. *69*, pp 31−69.
(18) Borges, I. Excited electronic and ionized states of the nitramide molecule, H_2NNO_2, studied by the symmetry adapted-cluster configuration method. *Theor. Chem. Acc.* **2008**, *121*, 239−246.
(19) Borges, I. Excited electronic and ionized states of *N,N*-dimethylnitramine. *Chem. Phys.* **2008**, *349*, 256−262.
(20) Borges, I., Jr. Electronic and ionization spectra of 1,1-diamino-2,2-dinitroethylene, FOX-7. *J. Mol. Model.* **2014**, *20* (3), 1−7.
(21) Borges, I.; Aquino, A. J.; Barbatti, M.; Lischka, H. The electronically excited states of RDX (hexahydro-1,3,5-trinitro-1,3,5-triazine): Vertical excitations. *Int. J. Quantum Chem.* **2009**, *109* (11), 2348−2355.
(22) Loos, K. R.; Gunthard, H. H. Infrared spectrum and internal-rotation barrier of nitroethylene. *J. Chem. Phys.* **1967**, *46* (3), 1200−&.
(23) Zhang, S. Q.; Wang, Y. Q.; Zheng, X. M. Density functional theory investigation of the photoisomerization reaction of nitroalkanes and nirroaromatic compounds. *Acta Phys.-Chim. Sin.* **2006**, *22* (12), 1489−1494.
(24) Shamov, A. G.; Khrapkovskii, G. M. A theoretical study of the gas-phase pyrolysis of nitroethylene. *Mendeleev Commun.* **2001**, *4*, 163−164.
(25) Khrapkovskii, G. M.; Shamov, A. G.; Nikolaeva, E. V.; Chachkov, D. V. Mechanisms of the gas-phase decomposition of C-nitro compounds inferred from quantum chemical calculations. *Russ. Chem. Rev.* **2009**, *78* (10), 903−943.
(26) Loos, K. R.; Wild, U. P.; Gunthard, H. H. Ultraviolet spectra and electronic structure of nitroethylene. *Spectrochim. Acta, Part A: Mol. Spectrosc.* **1969**, *A 25* (1), 275.
(27) Ha, T. K. Ab-initio SCF-CI study of electronic-spectra of nitroethylene. *Mol. Phys.* **1974**, *27* (3), 753−761.
(28) Borges, I.; Barbatti, M.; Aquino, A. J. A.; Lischka, H. Electronic spectra of nitroethylene. *Int. J. Quantum Chem.* **2012**, *112* (4), 1225−1232.
(29) Ben-Nun, M.; Martinez, T. J. Photodynamics of ethylene: Ab initio studies of conical intersections. *Chem. Phys.* **2000**, *259* (2−3), 237−248.
(30) Viel, A.; Krawczyk, R. P.; Manthe, U.; Domcke, W. Photoinduced dynamics of ethene in the N, V, and Z valence states: A six-dimensional nonadiabatic quantum dynamics investigation. *J. Chem. Phys.* **2004**, *120* (23), 11000−11010.
(31) Barbatti, M.; Paier, J.; Lischka, H. Photochemistry of ethylene: A multireference configuration interaction investigation of the excited-state energy surfaces. *J. Chem. Phys.* **2004**, *121* (23), 11614−11624.
(32) Barbatti, M.; Granucci, G.; Persico, M.; Lischka, H. Semiempirical molecular dynamics investigation of the excited state lifetime of ethylene. *Chem. Phys. Lett.* **2005**, *401* (1−3), 276−281.
(33) Fabiano, E.; Keal, T. W.; Thiel, W. Implementation of surface hopping molecular dynamics using semiempirical methods. *Chem. Phys.* **2008**, *349* (1−3), 334−347.
(34) Tao, H. L.; Levine, B. G.; Martinez, T. J. Ab Initio Multiple Spawning Dynamics Using Multi-State Second-Order Perturbation Theory. *J. Phys. Chem. A* **2009**, *113* (49), 13656−13662.
(35) Sellner, B.; Barbatti, M.; Muller, T.; Domcke, W.; Lischka, H. Ultrafast non-adiabatic dynamics of ethylene including Rydberg states. *Mol. Phys.* **2013**, *111* (16−17), 2439−2450.
(36) Barbatti, M.; Aquino, A. J. A.; Lischka, H. A multireference configuration interaction investigation of the excited-state energy surfaces of fluoroethylene (C_2H_3F). *J. Phys. Chem. A* **2005**, *109* (23), 5168−5175.
(37) Bonačić-Koutecký, V.; Koutecky, J.; Michl, J. Neutral and charged biradicals, zwitterions, funnels in s1, and proton translocation - Their role in photochemistry, photophysics, and vision. *Angew. Chem., Int. Ed. Engl.* **1987**, *26* (3), 170−189.
(38) Michl, J.; Bonačić-Koutecký, V. *Electronic Aspects of Organic Phtotochemistry*; Wiley: New York, 1990.
(39) Szalay, P. G.; Muller, T.; Gidofalvi, G.; Lischka, H.; Shepard, R. Multiconfiguration Self-Consistent Field and Multireference Configuration Interaction Methods and Applications. *Chem. Rev.* **2012**, *112* (1), 108−181.
(40) Bunge, A. Electronic wavefunctions for atoms 3. Partition of degenerate spaces and ground state of C. *J. Chem. Phys.* **1970**, *53* (1), 20−28.
(41) Langhoff, S. R.; Davidson, E. R. Configuration interaction calculations on nitrogen molecule. *Int. J. Quantum Chem.* **1974**, *8* (1), 61−72.
(42) Bruna, P. J.; Peyerimhoff, S. D.; Buenker, R. J. The ground-state of the CN^+ ion - A multi-reference CI study. *Chem. Phys. Lett.* **1980**, *72* (2), 278−284.
(43) Dill, J. D.; Pople, J. A. Self-consistent molecular-orbital methods 15. Extended gaussian-type basis sets for lithium, beryllium, and boron. *J. Chem. Phys.* **1975**, *62* (7), 2921−2923.
(44) Clark, T.; Chandrasekhar, J.; Spitznagel, G. W.; Schleyer, P. V. Efficient diffuse function-augmented basis sets for anion calculations. III. The 3-21+G basis set for first-row elements, Li−F. *J. Comput. Chem.* **1983**, *4* (3), 294−301.
(45) Frisch, M. J.; Pople, J. A.; Binkley, J. S. Self-consistent molecular-orbital methods 0.25. Supplementary functions for Gaussian-basis sets. *J. Chem. Phys.* **1984**, *80* (7), 3265−3269.
(46) Fogarasi, G.; Zhou, X. F.; Taylor, P. W.; Pulay, P. The calculation of ab initio molecular geometries - Efficient optimization by

natural internal coordinates and empirical correction by offset forces. *J. Am. Chem. Soc.* **1992**, *114* (21), 8191−8201.
(47) Csaszar, P.; Pulay, P. Geometry optimization by direct inversion in the iterative subspace. *J. Mol. Struct.* **1984**, *114* (MAR), 31−34.
(48) Shepard, R. Geometrical energy derivative evaluation with MRCI wave-functions. *Int. J. Quantum Chem.* **1987**, *31* (1), 33−44.
(49) Shepard, R.; Lischka, H.; Szalay, P. G.; Kovar, T.; Ernzerhof, M. A general multireference configuration−interaction gradient program. *J. Chem. Phys.* **1992**, *96* (3), 2085−2098.
(50) Yarkony, D. R. Conical intersections: Diabolical and often misunderstood. *Acc. Chem. Res.* **1998**, *31* (8), 511−518.
(51) Lischka, H.; Dallos, M.; Szalay, P. G.; Yarkony, D. R.; Shepard, R. Analytic evaluation of nonadiabatic coupling terms at the MR-CI level. I. Formalism. *J. Chem. Phys.* **2004**, *120* (16), 7322−7329.
(52) Dallos, M.; Lischka, H.; Shepard, R.; Yarkony, D. R.; Szalay, P. G. Analytic evaluation of nonadiabatic coupling terms at the MR-CI level. II. Minima on the crossing seam: Formaldehyde and the photodimerization of ethylene. *J. Chem. Phys.* **2004**, *120* (16), 7330−7339.
(53) Lischka, H.; Shepard, R.; Pitzer, R. M.; Shavitt, I.; Dallos, M.; Muller, T.; Szalay, P. G.; Seth, M.; Kedziora, G. S.; Yabushita, S.; et al. High-level multireference methods in the quantum-chemistry program system COLUMBUS: Analytic MR-CISD and MR-AQCC gradients and MR-AQCC-LRT for excited states, GUGA spin-orbit CI and parallel CI density. *Phys. Chem. Chem. Phys.* **2001**, *3* (5), 664−673.
(54) Lischka, H.; Müller, T.; Szalay, P. G.; Shavitt, I.; Pitzer, R. M.; Shepard, R. Columbus—A program system for advanced multi-reference theory calculations. *Wiley Interdiscip. Rev.: Comput. Mol. Sci.* **2011**, *1* (2), 191−199.
(55) Lischka, H.; Shepard, R.; Shavitt, I.; Pitzer, R. M.; Dallos, M.; Müller, T.; Szalay, P. G.; Brown, F. B.; Ahlrichs, R.; Chang, A.;et al. *COLUMBUS, an ab initio electronic structure program*, release 7.0, www.univie.ac.at/columbus, 2012.
(56) Dachsel, H.; Lischka, H.; Shepard, R.; Nieplocha, J.; Harrison, R. J. A massively parallel multireference configuration interaction program: The parallel COLUMBUS program. *J. Comput. Chem.* **1997**, *18* (3), 430−448.
(57) Muller, T. Large-Scale Parallel Uncontracted Multireference-Averaged Quadratic Coupled Cluster: The Ground State of the Chromium Dimer Revisited. *J. Phys. Chem. A* **2009**, *113* (45), 12729−12740.
(58) *DALTON, a molecular electronic structure program*, see http://daltonprogram.org/, 1.7; 1997.
(59) Salem, L. Theory of photochemical reactions. *Science* **1976**, *191* (4229), 822−830.
(60) Bonačić-Koutecký, V.; Bruckmann, P.; Hiberty, P.; Koutecky, J.; Leforestier, C.; Salem, L. Sudden polarization in zwitterionic Z1 excited-states of organic intermediates. Photochemical implications. *Angew. Chem., Int. Ed. Engl.* **1975**, *14* (8), 575−576.
(61) Klessinger, M.; Michl, J. *Excited States and Photochemistry of Organic Molecules*; VCH Publishers: New York, 1995.
(62) Atchity, G. J.; Xantheas, S. S.; Ruedenberg, K. Potential-energy surfaces near intersections. *J. Chem. Phys.* **1991**, *95* (3), 1862−1876.
(63) Domcke, W.; Yarkony, D. R.; Köppel, H. *Conical Intersections: Electronic Structure, Dynamics & Spectroscopy*; World Scientific: River Edge, NJ, 2004.
(64) Domcke, W. In *Conical Intersections: Electronic Structure, Dynamics & Spectroscopy*; Advanced Series in Physical Chemistry; Ng, C.-Y., Ed.; World Scientific: River Edge, NJ, 2004; p 395.